JOURNAL OF SOLID STATE CHEMISTRY **136,** 93–102 (1998)
ARTICLE NO. SC977665

# Two New 1,3-Diammonium-Propane Zinc Hydrogen Phosphates: $H_3N(CH_2)_3NH_3 \cdot Zn_2(HPO_4)_2(H_2PO_4)_2$, with 12-Ring Layers, and $H_3N(CH_2)_3NH_3 \cdot Zn(HPO_4)_2$, with 4-Ring Ladders

William T. A. Harrison,[1] Zsolt Bircsak, Lakshitha Hannooman, and Zhenghua Zhang

*Department of Chemistry, University of Western Australia, Nedlands, Western Australia 6907, Australia*
E-mail: wtah@chem.uwa.edu.au

Received July 9, 1997; in revised form October 1, 1997; accepted October 20, 1997

**The solution-mediated syntheses, single-crystal structures, and some physical properties of the first 1,3-diammonium-propane zinc phosphates, $H_3N(CH_2)_3NH_3 \cdot Zn_2(HPO_4)_2(H_2PO_4)_2$ and $H_3N(CH_2)_3NH_3 \cdot Zn(HPO_4)_2$, are described. Both phases contain vertex-sharing $ZnO_4$ and $(H_2/H)PO_4$ tetrahedra, accompanied by doubly protonated organic cations. $H_3N(CH_2)_3NH_3 \cdot Zn_2(HPO_4)_2(H_2PO_4)_2$ consists of a layered motif of infinite sheets of tetrahedral 12-rings, whereas $H_3N(CH_2)_3NH_3 \cdot Zn(HPO_4)_2$ is strongly one-dimensional and consists of tetrahedral 4-ring "ladders." Crystal data: $H_3N(CH_2)_3NH_3 \cdot Zn_2(HPO_4)_2(H_2PO_4)_2$, $M_r = 590.82$, monoclinic, space group $P2_1/a$ (No. 14), $a = 15.056(2)$ Å, $b = 7.8454(8)$ Å, $c = 16.344(2)$ Å, $\beta = 115.469(8)^\circ$, $V = 1742.9(3)$ Å$^3$, $Z = 4$, $R(F) = 5.17\%$, $R_w(F) = 5.68\%$ [2859 observed reflections with $I = 3\sigma(I)$]; $H_3N(CH_2)_3NH_3 \cdot Zn(HPO_4)_2$, $M_r = 333.48$, orthorhombic, space group $P2_12_12_1$ (No. 19), $a = 5.2206(7)$ Å, $b = 12.717(2)$ Å, $c = 15.570(2)$ Å, $V = 1033.7(3)$ Å$^3$, $Z = 4$, $R(F) = 4.16\%$, $R_w(F) = 3.75\%$ [1491 observed reflections with $I > 3\sigma(I)$].**


## INTRODUCTION

Several open-framework zincophosphates (ZnPOs) templated by organic cations have recently been reported (1–11). Their crystal structures are strongly dependent on the identity of the structure-directing organic species and display interesting features such as tetrahedral 3-rings (2, 4) and infinite chains of –Zn–O–Zn–O– bonds (7). $ZnPO_4 \cdot \frac{1}{2} C_2N_2H_{10}$ (8) is notable for its saturated, zeolite-like, fully alternating Zn/P framework topology. Some structure-directing species such as the tetramethylammonium (9) and guanidinium cations (10, 11) appear to preferentially template novel large-pore ZnPO frameworks with exceptionally low framework densities.

[1] To whom correspondence should be addressed.

Here, we report the solution-mediated syntheses and single-crystal structures of two new 1,3-diammonium-propane ($[HN_3(CH_2)_3NH_3]^{2+}$) zincophosphates. It is known that such linear-chain bifunctional amines are effective in templating other types of novel structures such as vanadophosphates and ferrophosphates (12, 13). Here we show that $H_3N(CH_2)_3NH_3 \cdot Zn_2(HPO_4)_2(H_2PO_4)_2$ adopts a layered structure containing tetrahedral zincophosphate 12-rings, whereas $H_3N(CH_2)_3NH_3 \cdot Zn(HPO_4)_2$ shows strong one-dimensional character and is built up from 4-ring "ladders."

## EXPERIMENTAL

### *Synthesis*

$H_3N(CH_2)_3NH_3 \cdot Zn_2(HPO_4)_2(H_2PO_4)_2$ was prepared as follows: 85% phosphoric acid (8.45 g), 1,3-diaminopropane (1.774 g), and zinc oxide (1.00 g) were placed in an unsealed 23-ml Teflon pot and heated at 95°C for 24 hr. Upon cooling, transparent, platy crystals were recovered by vacuum filtration and washing with cold water. $H_3N(CH_2)_3NH_3 \cdot Zn(HPO_4)_2$ was prepared from the same starting materials heated to 160°C for 48 hr in sealed Teflon pot. An estimated pressure of 10 atm was achieved. After cooling, a mass of clear needles was recovered by vacuum filtration and washing with cold water. Both products appear to be completely stable when stored in dry air.

### *Physical Characterization*

Powder X-ray data for well-ground, white powder samples of the title compounds were collected on a Siemens D5000 automated powder diffractometer [Cu$K\alpha$ radiation, $\lambda = 1.54178$ Å, $T = 25(2)$°C]. A software "stripping" and peak-fitting routine established peak positions relative to Cu$K\alpha_1$ ($\lambda = 1.54056$ Å), and *hkl* indices were assigned by comparison with LAZY-PULVERIX (14) simulations of the single-crystal structures (*vide infra*). The least-squares refinements were performed by using the program UNITCELL



0022-4596/98 $25.00

(15). For $H_3N(CH_2)_3NH_3 \cdot Zn_2(HPO_4)_2(H_2PO_4)_2$: monoclinic, $a = 15.057(9)$ Å, $b = 7.859(4)$ Å, $c = 16.344(7)$ Å, $\beta = 115.50(5)^\circ$, $V = 1745(2)$ Å$^3$. For $H_3N(CH_2)_3NH_3 \cdot Zn(HPO_4)_2$: orthorhombic, $a = 5.222(3)$ Å, $b = 12.716(7)$ Å, $c = 15.559(6)$ Å, $V = 1033(2)$ Å$^3$. Powder data for $H_3N(CH_2)_3NH_3 \cdot Zn_2(HPO_4)_2(H_2PO_4)_2$ and $H_3N(CH_2)_3NH_3 \cdot Zn(HPO_4)_2$ are listed in Tables 1 and 2, respectively. Thermogravimetric analysis (TGA) was performed on a Rigaku Thermoflex instrument (ramp at 20°C/min under oxygen).

*Single-Crystal Structure Determinations*

In each case a suitable crystal [$H_3N(CH_2)_3NH_3 \cdot Zn_2(HPO_4)_2(H_2PO_4)_2$: transparent plate, $\sim 0.1 \times 0.5 \times 0.5$ mm; $H_3N(CH_2)_3NH_3 \cdot Zn(HPO_4)_2$: transparent rod, $\sim 0.02 \times 0.02 \times 0.5$ mm] was mounted on a thin glass fiber with cyanoacrylate adhesive, and room-temperature [25(2)°C] intensity data were collected on a Siemens P4 automated four-circle diffractometer (graphite-monochromated Mo$K\alpha$ radiation, $\lambda = 0.71073$ Å), as summarized in Table 3. The application of peak-search, centering, indexing, and least-squares refinement routines led to a monoclinic unit cell for $H_3N(CH_2)_3NH_3 \cdot Zn_2(HPO_4)_2(H_2PO_4)_2$ and an orthorhombic cell for $H_3N(CH_2)_3NH_3 \cdot Zn(HPO_4)_2$. There is a strong subcell for $H_3N(CH_2)_3NH_3 \cdot Zn_2(HPO_4)_2(H_2PO_4)_2$ based on a primitive monoclinic cell with $a = 8.396$ Å, $b = 7.855$ Å, $c = 13.285$ Å, and $\beta = 95.2^\circ$ (*vide infra*). Intensity data were collected using the $\omega$–$2\theta$ scan mode. Three standard reflections, remeasured every 100 observations, showed no significant variation in intensity over the course of each data collection. Crystal absorption [for $H_3N(CH_2)_3NH_3 \cdot Zn_2(HPO_4)_2(H_2PO_4)_2$, range of equivalent transmission factors = 0.42–0.57; for $H_3N(CH_2)_3NH_3 \cdot Zn(HPO_4)_2$, 0.49–0.61] was accounted for by $\psi$ scans. Data merging for $H_3N(CH_2)_3NH_3 \cdot Zn_2(HPO_4)_2(H_2PO_4)_2$ resulted in 3248 reflections ($R_{Int} = 3.82\%$), with 2859 of these observed according to the criterion $I > 3\sigma(I)$; the systematic absences ($h0l$, $h \neq 2n$; $0k0$, $k \neq 2n$) indicated space group $P2_1/a$ (non-standard setting of $P2_1/c$, No. 14). The systematic absence conditions in the reduced data for $H_3N(CH_2)_3NH_3 \cdot Zn(HPO_4)_2$ ($h00$, $h \neq 2n$; $0k0$, $k \neq 2n$; $00l$,

**TABLE 1**
**Powder X-Ray Data for $H_3N(CH_2)_3NH_3 \cdot Zn_2(HPO_4)_2(H_2PO_4)_2$**

| $h$ | $k$ | $l$ | $d_{obs}$ (Å) | $d_{calc}$ (Å) | $\Delta d$ | $I_{rel}$ |
|---|---|---|---|---|---|---|
| 0 | 0 | 2 | 7.380 | 7.376 | 0.004 | 100 |
| 1 | 1 | −1 | 6.766 | 6.754 | 0.012 | 7 |
| 1 | 1 | −2 | 5.634 | 5.642 | −0.008 | < 1 |
| 0 | 1 | 2 | 5.367 | 5.377 | −0.010 | < 1 |
| 2 | 1 | 0 | 5.150 | 5.139 | 0.010 | 6 |
| 2 | 1 | −2 | 5.060 | 5.060 | 0.000 | 12 |
| 0 | 0 | 3 | 4.921 | 4.917 | 0.003 | < 1 |
| 3 | 1 | −1 | 4.195 | 4.202 | −0.007 | 21 |
| 2 | 0 | −4 | 4.057 | 4.055 | 0.002 | 37 |
| 0 | 2 | 0 | 3.929 | 3.928 | 0.002 | 8 |
| 1 | 2 | −1 | 3.762 | 3.765 | −0.004 | 6 |
| 2 | 1 | 2 | 3.687 | 3.691 | −0.004 | 33 |
| 2 | 1 | −4 | 3.606 | 3.603 | 0.003 | 10 |
| 1 | 2 | 1 | 3.554 | 3.555 | −0.001 | 7 |
| 0 | 2 | 2 | 3.465 | 3.467 | −0.002 | 6 |
| 4 | 0 | 0 | 3.395 | 3.398 | −0.002 | 17 |
| 4 | 0 | −4 | 3.306 | 3.307 | 0.000 | 53 |
| 2 | 0 | −5 | 3.269 | 3.269 | 0.000 | 4 |
| 1 | 2 | −3 | 3.184 | 3.183 | 0.001 | 7 |
| 4 | 1 | 0 | 3.120 | 3.119 | 0.001 | 5 |
| 3 | 2 | −1 | 3.081 | 3.082 | −0.002 | 3 |
| 4 | 1 | −4 | 3.047 | 3.048 | −0.001 | 5 |
| 3 | 1 | −5 | 2.945 | 2.944 | 0.001 | 2 |
| 2 | 2 | 2 | 2.863 | 2.863 | 0.000 | 2 |
| 2 | 2 | −4 | 2.821 | 2.821 | 0.000 | 12 |
| 5 | 1 | −3 | 2.789 | 2.790 | −0.001 | 3 |
| 3 | 2 | 1 | 2.762 | 2.763 | −0.001 | 4 |
| 4 | 2 | −2 | 2.716 | 2.717 | −0.001 | 7 |
| 4 | 0 | −6 | 2.590 | 2.591 | −0.001 | 9 |
| 5 | 1 | −5 | 2.505 | 2.507 | −0.002 | 5 |
| 0 | 0 | 6 | 2.458 | 2.459 | −0.001 | 16 |
| 6 | 1 | −4 | 2.349 | 2.347 | 0.002 | 5 |
| 1 | 3 | 3 | 2.204 | 2.206 | −0.002 | 9 |
| 2 | 1 | −8 | 1.9466 | 1.9491 | −0.0025 | 5 |
| 0 | 0 | 8 | 1.8435 | 1.8440 | −0.0005 | 5 |
| 6 | 1 | −8 | 1.8268 | 1.8285 | −0.0017 | 4 |

**TABLE 2**
**Powder X-Ray Data for $H_3N(CH_2)_3NH_3 \cdot Zn(HPO_4)_2$**

| $h$ | $k$ | $l$ | $d_{obs}$ (Å) | $d_{calc}$ (Å) | $\Delta d$ | $I_{rel}$ |
|---|---|---|---|---|---|---|
| 0 | 1 | 1 | 9.841 | 9.846 | −0.006 | 100 |
| 0 | 0 | 2 | 7.777 | 7.780 | −0.002 | 46 |
| 0 | 1 | 2 | 6.647 | 6.636 | 0.010 | 7 |
| 0 | 2 | 1 | 5.882 | 5.886 | −0.003 | 4 |
| 1 | 0 | 1 | 4.947 | 4.951 | −0.003 | 3 |
| 0 | 1 | 3 | 4.806 | 4.802 | 0.004 | 17 |
| 1 | 1 | 1 | 4.620 | 4.613 | 0.006 | 4 |
| 1 | 1 | 2 | 4.099 | 4.104 | −0.005 | 5 |
| 1 | 2 | 0 | 4.033 | 4.035 | −0.002 | 1 |
| 1 | 0 | 3 | 3.682 | 3.680 | 0.002 | 6 |
| 1 | 2 | 2 | 3.586 | 3.582 | 0.004 | 3 |
| 1 | 1 | 3 | 3.536 | 3.535 | 0.001 | 7 |
| 0 | 3 | 3 | 3.283 | 3.282 | 0.001 | 46 |
| 1 | 3 | 1 | 3.221 | 3.220 | 0.001 | 5 |
| 1 | 2 | 3 | 3.182 | 3.185 | −0.002 | 14 |
| 1 | 0 | 4 | 3.117 | 3.119 | −0.002 | 6 |
| 1 | 1 | 4 | 3.030 | 3.030 | 0.000 | 4 |
| 0 | 4 | 2 | 2.942 | 2.943 | −0.001 | 10 |
| 1 | 2 | 4 | 2.800 | 2.801 | −0.001 | 6 |
| 1 | 1 | 5 | 2.615 | 2.616 | −0.001 | 3 |
| 0 | 0 | 6 | 2.595 | 2.593 | 0.001 | 5 |
| 2 | 0 | 1 | 2.576 | 2.575 | 0.001 | 1 |
| 1 | 3 | 4 | 2.512 | 2.512 | −0.001 | 2 |
| 1 | 2 | 5 | 2.463 | 2.464 | −0.002 | 7 |
| 1 | 4 | 4 | 2.226 | 2.227 | 0.000 | 3 |
| 0 | 2 | 7 | 2.098 | 2.098 | 0.000 | 3 |
| 1 | 4 | 6 | 1.876 | 1.875 | 0.001 | 2 |

**TABLE 3**
**Crystallographic/Data Collection Parameters**

| $H_3N(CH_2)_3NH_3 \cdot Zn_2(HPO_4)_2(H_2PO_4)_2$ | $H_3N(CH_2)_3NH_3 \cdot Zn(HPO_4)_2$ |
|---|---|
| Emp formula | $Zn_2P_4O_{16}N_2C_3H_{18}$ | $Zn_1P_2O_8N_2C_3H_{14}$ |
| Formula wt | 590.82 | 333.48 |
| Crystal system | Monoclinic | Orthorhombic |
| $a$ (Å) | 15.056(2) | 5.2206(7) |
| $b$ (Å) | 7.8454(8) | 12.717(2) |
| $c$ (Å) | 16.344(2) | 15.570(2) |
| $\beta$ (deg) | 115.469(8) | 90 |
| $V$ (Å$^3$) | 1742.9(3) | 1033.7(3) |
| $Z$ | 4 | 4 |
| Space group | $P2_1/a$ (No. 14) | $P2_12_12_1$ (No. 19) |
| $T$ (°C) | 25(2) | 25(2) |
| $\lambda$(Mo$K\alpha$) (Å) | 0.71073 | 0.71073 |
| $\rho_{calc}$ (g/cm$^3$) | 2.25 | 2.14 |
| $\mu$ (cm$^{-1}$) | 32.65 | 27.67 |
| Total data | 5429 | 2034 |
| Observed data[a] | 2859 | 1491 |
| Parameters | 246 | 148 |
| $R(F)$[b] | 5.17 | 4.16 |
| $R_w(F)$[c] | 5.68 | 3.75 |

[a] $I > 3\sigma(I)$ after data merging.
[b] $R = 100 \times \sum ||F_o| - |F_c|| / \sum |F_o|$.
[c] $R_w = 100 \times [\sum w(|F_o| - |F_c|)^2 / \sum w|F_o|^2]^{1/2}$.

$l \neq 2n$) indicated space group $P2_12_12_1$ (No. 19), with $R_{Int} = 2.89\%$ for 1547 merged reflections (1491 observed).

For $H_3N(CH_2)_3NH_3 \cdot Zn_2(HPO_4)_2(H_2PO_4)_2$, approximate positional parameters for the Zn, P, and some O atoms were located by direct methods using the program SIR92 (16) and the crystal structure model was successfully developed in space group $P2_1/a$. The remaining O, N, and C atom positions were readily located from difference Fourier maps. No proton positions could be located from difference maps. Protons associated with the doubly protonated 1,3-diaminopropane molecule were located geometrically [$d$(N–H) = 0.95 Å, $d$(C–H) = 0.95 Å] and refined by riding on their N and C atoms. The final cycles of full-matrix least-squares refinement [program CRYSTALS (17)], using complex, neutral-atom scattering factors (18), minimized the function $\sum w_i(F_o - F_c)^2$, with $w_i = 1/[\sigma(F)]^2$, and included anisotropic temperature factors for all the nonhydrogen atoms and a Larson-type secondary extinction correction (19).

For $H_3N(CH_2)_3NH_3 \cdot Zn(HPO_4)_2$, starting Zn and P atom coordinates were located by direct methods, and the structure was developed in space group $P2_12_12_1$ (No. 19). The other non-hydrogen atoms were located from difference maps and added to the refinement. No proton positions could be located; those H atoms associated with the 1,3-diaminopropane species were placed geometrically and refined as for $H_3N(CH_2)_3NH_3 \cdot Zn_2(HPO_4)_2(H_2PO_4)_2$. The absolute structure of the individual crystal studied was established by refining the Flack parameter (20) to $-0.01$ (1) and is as listed in the results section. Assuming the opposite absolute structure (Flack parameter fixed at 1.00) resulted in significantly higher residuals of $R = 5.19\%$ and $R_w = 5.64\%$. Supplementary tables of hydrogen atom coordinates, anisotropic thermal factors, and observed and calculated structure factors for these materials are available from the authors.

## RESULTS

### *Crystal Structure of $H_3N(CH_2)_3NH_3 \cdot Zn_2(HPO_4)_2(H_2PO_4)_2$*

Final atomic positional and thermal parameters for $H_3N(CH_2)_3NH_3 \cdot Zn_2(HPO_4)_2(H_2PO_4)_2$ are listed in Table 4, with selected bond distance and bond angle data in Table 5. $H_3N(CH_2)_3NH_3 \cdot Zn_2(HPO_4)_2(H_2PO_4)_2$ is a new organozincophosphate consisting of a structure with strong two-dimensional character based on sheets of $ZnO_4$, $HPO_4$, and $H_2PO_4$ tetrahedra fused together via Zn–O–P bonds. A CAMERON (21) view of the asymmetric unit of $H_3N(CH_2)_3NH_3 \cdot Zn_2(HPO_4)_2(H_2PO_4)_2$ is shown in Fig. 1, and the complete crystal structure in Fig. 2.

**TABLE 4**
**Atomic Coordinates and Thermal Factors for $H_3N(CH_2)_3NH_3 \cdot Zn_2(HPO_4)_2(H_2PO_4)_2$**

| Atom | $x$ | $y$ | $z$ | $U_{eq}$[a] |
|---|---|---|---|---|
| Zn(1) | 0.11070(6) | 0.3331(1) | 0.50544(5) | 0.0174 |
| Zn(2) | −0.10564(6) | 0.8347(1) | 0.01006(5) | 0.0192 |
| P(1) | 0.1798(1) | −0.0565(3) | 0.4782(1) | 0.0169 |
| P(2) | 0.0545(1) | 0.4733(3) | 0.6610(1) | 0.0181 |
| P(3) | −0.0854(1) | 0.9896(3) | −0.1610(1) | 0.0200 |
| P(4) | −0.3237(1) | 0.9411(3) | −0.0300(1) | 0.0191 |
| O(1) | 0.1429(4) | 0.0936(7) | 0.5133(3) | 0.0231 |
| O(2) | −0.0059(4) | 0.3702(7) | 0.3944(3) | 0.0280 |
| O(3) | 0.2170(3) | 0.4824(7) | 0.5139(4) | 0.0228 |
| O(4) | 0.0802(4) | 0.3393(8) | 0.6087(3) | 0.0254 |
| O(5) | 0.1091(4) | −0.1035(7) | 0.3823(3) | 0.0259 |
| O(6) | 0.1855(4) | −0.2056(7) | 0.5443(3) | 0.0246 |
| O(7) | −0.0201(4) | 0.3851(7) | 0.6940(4) | 0.0258 |
| O(8) | 0.1433(3) | 0.5267(7) | 0.7466(3) | 0.0247 |
| O(9) | −0.0804(4) | 0.8489(7) | −0.0970(3) | 0.0254 |
| O(10) | −0.1232(4) | 0.5935(8) | 0.0191(4) | 0.0297 |
| O(11) | 0.0024(4) | 0.8836(8) | 0.1243(3) | 0.0301 |
| O(12) | −0.2183(3) | 0.9829(7) | −0.0125(3) | 0.0247 |
| O(13) | −0.3259(4) | 0.8060(8) | 0.0397(3) | 0.0285 |
| O(14) | −0.3788(4) | 0.8550(8) | −0.1233(3) | 0.0304 |
| O(15) | −0.1816(4) | 1.0973(8) | −0.1919(3) | 0.0295 |
| O(16) | −0.0880(4) | 0.8987(8) | −0.2473(3) | 0.0278 |
| N(1) | −0.4077(5) | 0.986(1) | 0.1741(4) | 0.0371 |
| N(2) | −0.0802(4) | 1.0320(9) | 0.3495(4) | 0.0257 |
| C(1) | −0.3107(6) | 0.999(1) | 0.2497(5) | 0.0349 |
| C(2) | −0.2398(6) | 1.092(1) | 0.2200(6) | 0.0339 |
| C(3) | −0.1413(6) | 1.007(1) | 0.2522(5) | 0.0337 |

[a] $U_{eq}$ (Å$^2$) = $\frac{1}{3}[U_1 + U_2 + U_3]$

**TABLE 5**
**Selected Bond Distances (Å) and Angles (°) for $H_3N(CH_2)_3NH_3 \cdot Zn_2(HPO_4)_2(H_2PO_4)_2$**

| | | | |
|---|---|---|---|
| Zn(1)–O(1) | 1.931(6) | Zn(1)–O(2) | 1.929(5) |
| Zn(1)–O(3) | 1.939(5) | Zn(1)–O(4) | 1.930(4) |
| Zn(2)–O(9) | 1.948(5) | Zn(2)–O(10) | 1.925(6) |
| Zn(2)–O(11) | 1.915(5) | Zn(2)–O(12) | 1.956(5) |
| P(1)–O(1) | 1.515(5) | P(1)–O(3) | 1.534(5) |
| P(1)–O(5) | 1.514(5) | P(1)–O(6) | 1.570(5) |
| P(2)–O(2) | 1.514(6) | P(2)–O(4) | 1.508(5) |
| P(2)–O(7) | 1.598(5) | P(2)–O(8) | 1.521(5) |
| P(3)–O(9) | 1.501(5) | P(3)–O(11) | 1.505(6) |
| P(3)–O(15) | 1.561(6) | P(3)–O(16) | 1.566(5) |
| P(4)–O(10) | 1.491(6) | P(4)–O(12) | 1.523(5) |
| P(4)–O(13) | 1.567(5) | P(4)–O(14) | 1.543(5) |
| O(1)–H(6) | 1.986(7) | O(2)–H(5) | 1.883(9) |
| O(5)–H(4) | 1.890(8) | O(7)–H(1) | 2.067(8) |
| O(9)–H(2) | 2.182(9) | O(13)–H(3) | 2.323(9) |
| N(1)–C(1) | 1.46(1) | N(2)–C(3) | 1.468(9) |
| C(1)–C(2) | 1.53(1) | C(2)–C(3) | 1.50(1) |
| Zn(1)–O(1)–P(1) | 148.5(3) | Zn(1)–O(2)–P(2) | 134.1(4) |
| Zn(1)–O(3)–P(1) | 131.4(3) | Zn(1)–O(4)–P(2) | 136.8(4) |
| Zn(2)–O(9)–P(3) | 134.2(4) | Zn(2)–O(10)–P(4) | 153.7(4) |
| Zn(2)–O(11)–P(3) | 137.1(3) | Zn(2)–O(12)–P(4) | 131.0(4) |

There are 27 distinct nonhydrogen atoms in $H_3N(CH_2)_3NH_3 \cdot Zn_2(HPO_4)_2(H_2PO_4)_2$, all of which occupy general positions in the unit cell. The two zinc atoms have typical geometrical parameters, with $d_{av}$[Zn(1)–O] = 1.932(3) Å and $d_{av}$[Zn(2)–O] = 1.936(3) Å. Both zinc atoms make four Zn–O–P linkages to nearby phosphorus atoms. All four P atoms form the centers of tetrahedral phosphate groups, with $d_{av}$[P(1)–O] = 1.533(3) Å, $d_{av}$[P(2)–O] = 1.535 (3) Å, $d_{av}$[P(3)–O] = 1.533(3) Å, and $d_{av}$[P(4)–O] = 1.531(3) Å. Each of these dihydrogen/hydrogen phosphate entities participates in two P–O–Zn links and has two terminal P–O bonds. Assuming that the organic species is doubly protonated, six "framework" protons are required for charge-balancing purposes. We presume that these protons are located on some of the terminal P–O vertices, as found for similar organozincophosphates (1, 6, 11). Although these framework protons were not located in the crystal structure determination, some insight into their location is provided by variations in terminal P–O bond lengths (22) and individual P–O bond valences (23), suggesting that P(1)- and P(2)-centered moieties are hydrogen phosphate groups and that P(3)- and P(4)-centered moieties are dihydrogen phosphate groups. The 16 distinct oxygen atoms thus divide into eight Zn–O–P bridges with a fairly wide spread of angles [$\theta_{av} = 137.7°$] and eight terminal P–O vertices, six of which [O(6), O(7), O(13), O(14), O(15), and O(16)] are protonated. N–C and C–C geometrical parameters for the 1,3-diammonium-propane cation are typical (24).

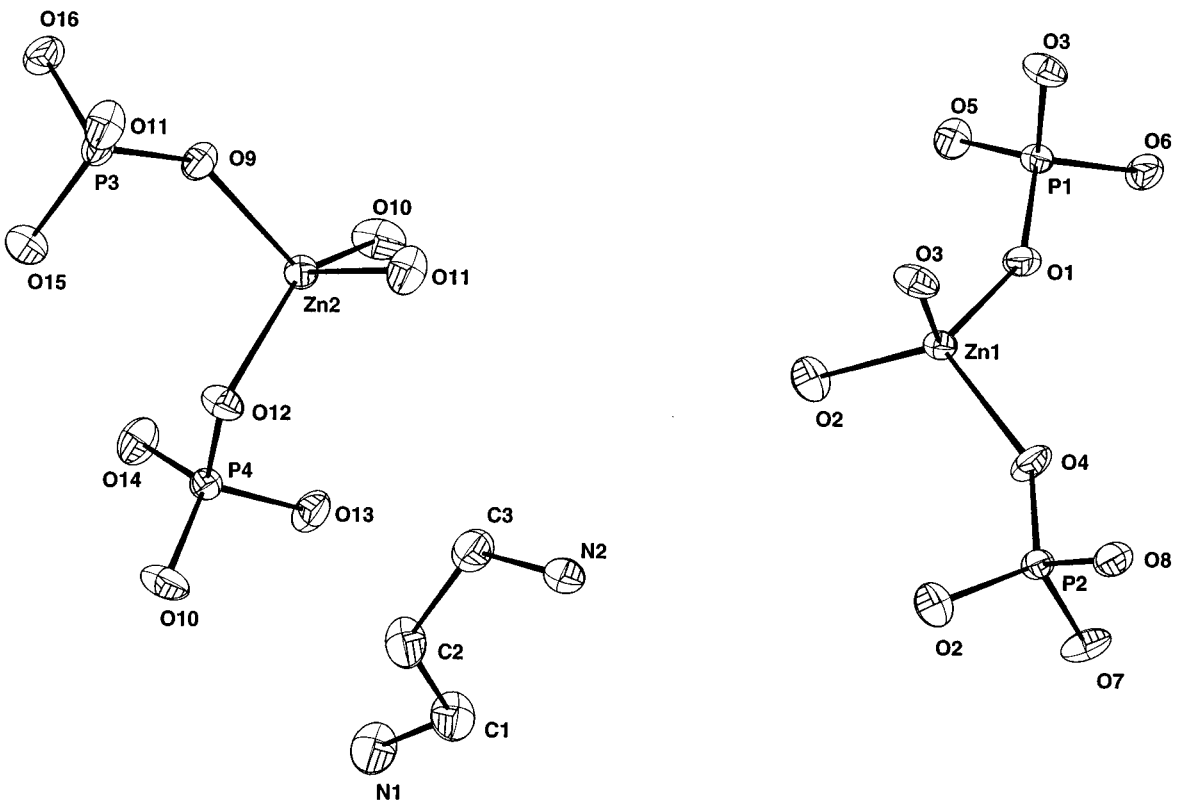


**FIG. 1.** Fragment of the $H_3N(CH_2)_3NH_3 \cdot Zn_2(HPO_4)_2(H_2PO_4)_2$ crystal structure (50% thermal ellipsoids) showing the atom-labeling scheme.

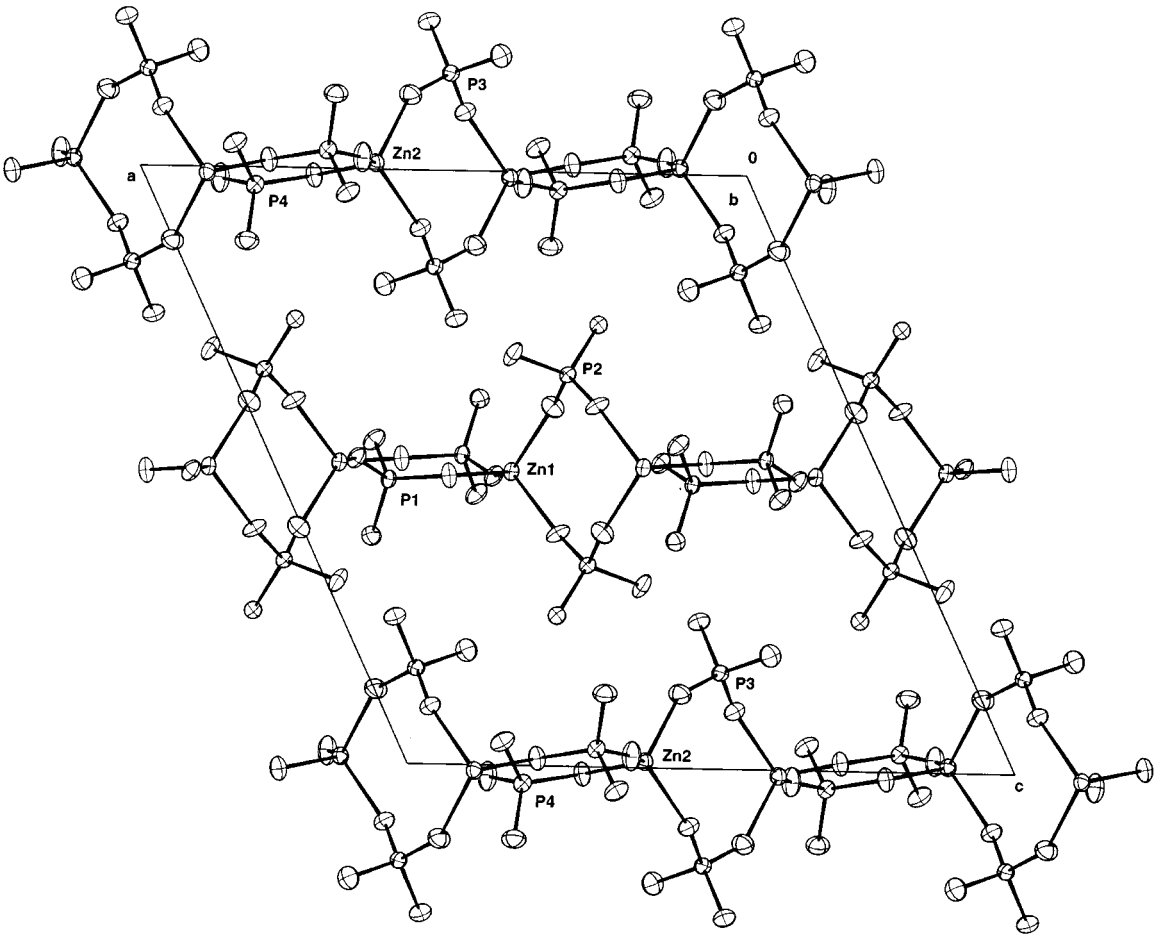


**FIG. 2.** View down [010] of the $H_3N(CH_2)_3NH_3 \cdot Zn_2(HPO_4)_2(H_2PO_4)_2$ crystal structure with the organic species omitted for clarity. Note the pseudosymmetry of the two distinct ZnPO layers.

The polyhedral connectivity in $H_3N(CH_2)_3NH_3 \cdot Zn_2(HPO_4)_2(H_2PO_4)_2$ results in a layered topology based on a two-dimensional network of squashed, "bifurcated" 12-rings (25). The 12-rings consist of 12 nodal tetrahedral atoms (6 Zn and 6 P, strictly alternating), or 24 atoms in total (Zn, P, and 12 oxygen atoms). There are two alternating, crystallographically distinct layers [nodal atoms Zn(1), P(1), and P(2) for the first layer and Zn(2), P(3), and P(4) for the second layer], both of which are aligned in the *ab* plane. Based on the assignment of framework proton positions noted earlier, one layer contains both hydrogen phosphate groups, and the other contains both dihydrogen phosphate groups. Each layer may be considered to be formed from a 4-ring built up from two $ZnO_4$ and two $(H/H_2)PO_4$ tetrahedra, fused through Zn–O–P vertices. These four rings are linked into continuous sheets via the second $(H/H_2)PO_4$ group through Zn–O–P bonds. This results in an infinite sheet of "bifurcated" 12-rings (Fig. 3); both distinct sheets have essentially the same structure. There are probably *intra*layer, and possibly *inter*layer, hydrogen bonds of the form P–OH $\cdots$ O as observed in other organozincophosphates such as $CN_3H_6 \cdot Zn_2(HPO_4)_2H_2PO_4$ (10).

The 1,3-diammonium-propane cations occupy interlayer sites and bond to the zincophosphate layers through N–H $\cdots$ O hydrogen bonds (Fig. 4). Based on the geometrical placement of the hydrogen atoms, all six N–H protons are involved in such linkages (Table 5), with bonds being made to acceptor oxygen species which are variously parts of Zn–O–P, P–O, and P–OH bonds. Thus, at first sight, there appears to be a strong correlation between the sheet structure and the guest–framework interactions; the 1,3-diammonium-propane cation might be templating 12-ring windows in the zincophosphate sheets as a result of its hydrogen-bonding interactions. Torsion angles of $-135.2^\circ$ for the N(1)–C(1)–C(2)–C(3) and $-73.8^\circ$ for the C(1)–C(2)–C(3)– N(2) groupings of the 1,3-diammonium-propane chain result.

The subcell noted eariler, with approximately half the volume of the actual unit cell, results in a structure with only a single crystallographically distinct zincophosphate

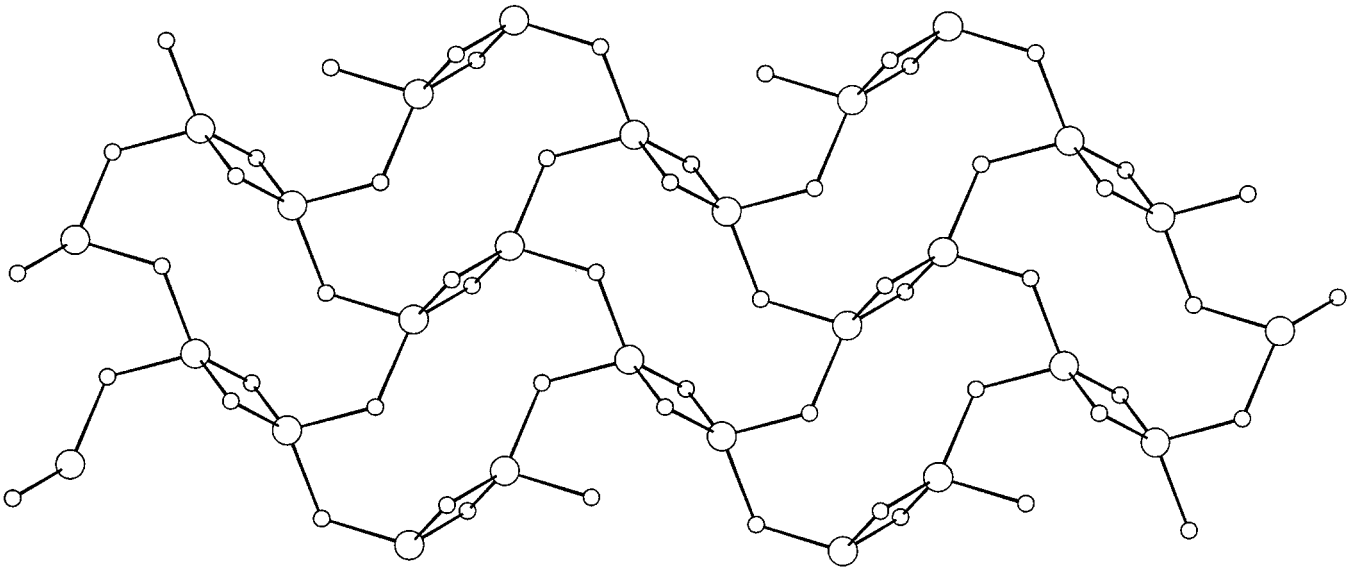

**FIG. 3.** Topological [zinc (large circles) to phosphorus (small circles)] connectivity of a zincophosphate layer in $H_3N(CH_2)_3NH_3 \cdot Zn_2(HPO_4)_2(H_2PO_4)_2$ showing the bifurcated 12-rings.

layer. However, this subcell model results in twofold disorder of one of the (di)hydrogen phosphate groups and unresolvable disorder of the 1,3-diammonium-propane species.

*Crystal Structure of* $H_3N(CH_2)_3NH_3 \cdot Zn(HPO_4)_2$

Final atomic positional and thermal parameters for $H_3N(CH_2)_3NH_3 \cdot Zn(HPO_4)_2$ are listed in Table 6, with

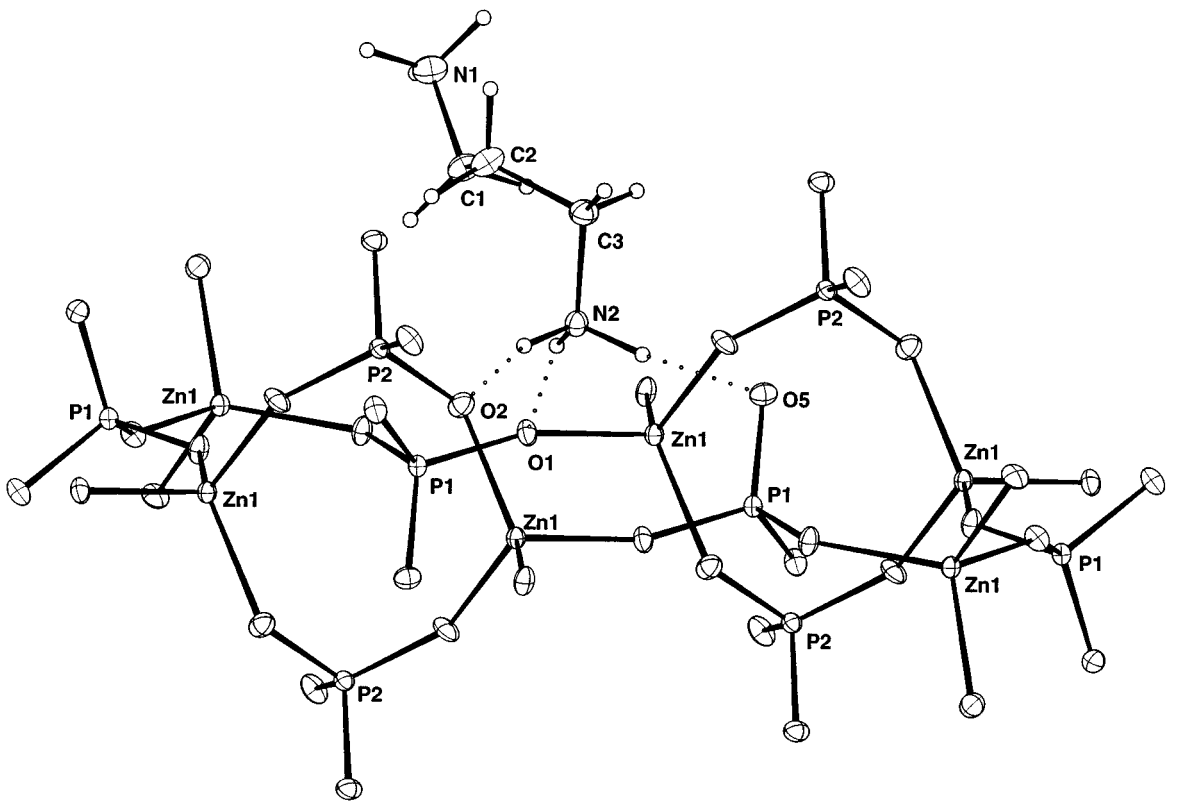


**FIG. 4.** Detail of the $H_3N(CH_2)_3NH_3 \cdot Zn_2(HPO_4)_2(H_2PO_4)_2$ structure showing the interaction of a 1,3-diammonium-propane cation with a zincophosphate tetrahedral 12-ring. Cation to framework H bonds are indicated by dotted lines (20% thermal ellipsoids).

**TABLE 6**
**Atomic Coordinates and Thermal Factors for $H_3N(CH_2)_3NH_3 \cdot Zn(HPO_4)_2$**

| Atom | *x* | *y* | *z* | $U_{eq}$[a] |
|---|---|---|---|---|
| Zn(1) | −0.1148(2) | 0.62822(6) | −0.04427(5) | 0.0149 |
| P(1) | 0.3815(4) | 0.6292(1) | 0.0685(1) | 0.0130 |
| P(2) | 0.1021(4) | 0.4173(1) | −0.1333(1) | 0.0144 |
| O(1) | 0.0947(9) | 0.6168(4) | 0.0582(3) | 0.0151 |
| O(2) | −0.046(1) | 0.7616(3) | −0.1001(3) | 0.0174 |
| O(3) | −0.043(1) | 0.5182(4) | −0.1259(3) | 0.0183 |
| O(4) | −0.4745(8) | 0.6011(4) | −0.0157(3) | 0.0134 |
| O(5) | 0.3373(9) | 0.4180(4) | −0.0671(3) | 0.0224 |
| O(6) | −0.057(1) | 0.3217(4) | −0.1085(3) | 0.0210 |
| O(7) | 0.216(1) | 0.4064(4) | −0.2240(3) | 0.0201 |
| O(8) | 0.4742(9) | 0.5482(4) | 0.1378(3) | 0.0158 |
| N(1) | 0.342(1) | 0.7835(4) | −0.2378(4) | 0.0210 |
| N(2) | 0.782(1) | 0.6420(4) | −0.4389(3) | 0.0211 |
| C(1) | 0.403(2) | 0.6691(5) | −0.2296(5) | 0.0261 |
| C(2) | 0.623(2) | 0.6395(6) | −0.2897(4) | 0.0226 |
| C(3) | 0.547(1) | 0.6488(6) | −0.3841(4) | 0.0188 |

[a] $U_{eq}$ (Å$^2$) = $\frac{1}{3}[U_1 + U_2 + U_3]$.

**TABLE 7**
**Selected Bond Distances (Å) and Angles (°) for $H_3N(CH_2)_3NH_3 \cdot Zn(HPO_4)_2$**

| | | | |
|---|---|---|---|
| Zn(1)–O(1) | 1.940(4) | Zn(1)–O(2) | 1.940(5) |
| Zn(1)–O(3) | 1.927(5) | Zn(1)–O(4) | 1.961(4) |
| P(1)–O(1) | 1.514(5) | P(1)–O(2) | 1.521(5) |
| P(1)–O(4) | 1.553(4) | P(1)–O(8) | 1.568(5) |
| P(2)–O(3) | 1.496(5) | P(2)–O(5) | 1.603(5) |
| P(2)–O(6) | 1.523(5) | P(2)–O(7) | 1.538(5) |
| O(2)–H(1) | 2.051(8) | O(6)–H(3) | 1.924(8) |
| O(6)–H(4) | 1.954(7) | O(6)–H(5) | 1.811(7) |
| O(7)–H(2) | 2.009(8) | O(8)–H(6) | 2.025(7) |
| N(1)–C(1) | 1.494(8) | N(2)–C(3) | 1.499(8) |
| C(1)–C(2) | 1.53(1) | C(2)–C(3) | 1.527(9) |
| Zn(1)–O(1)–P(1) | 129.5(3) | Zn(1)–O(2)–P(1) | 127.4(3) |
| Zn(1)–O(3)–P(2) | 140.5(3) | Zn(1)–O(4)–P(1) | 127.9(3) |

selected bond distance and bond angle data in Table 7. $H_3N(CH_2)_3NH_3 \cdot Zn(HPO_4)_2$ is a new phase with strong one-dimensional character consisting of infinite zincophosphate chains cross-linked by hydrogen-bonded 1,3-diammonium-propane cations. The bonding unit of $H_3N(CH_2)_3NH_3 \cdot Zn(HPO_4)_2$ is shown in Fig. 5, and the complete crystal structure in Fig. 6.

The single distinct zinc atom in $H_3N(CH_2)_3NH_3 \cdot Zn(HPO_4)_2$ is tetrahedral, with an average Zn–O bond length of 1.942(2) Å. Each of its four O atom partners also bonds to P, resulting in an average Zn–O–P bond angle of

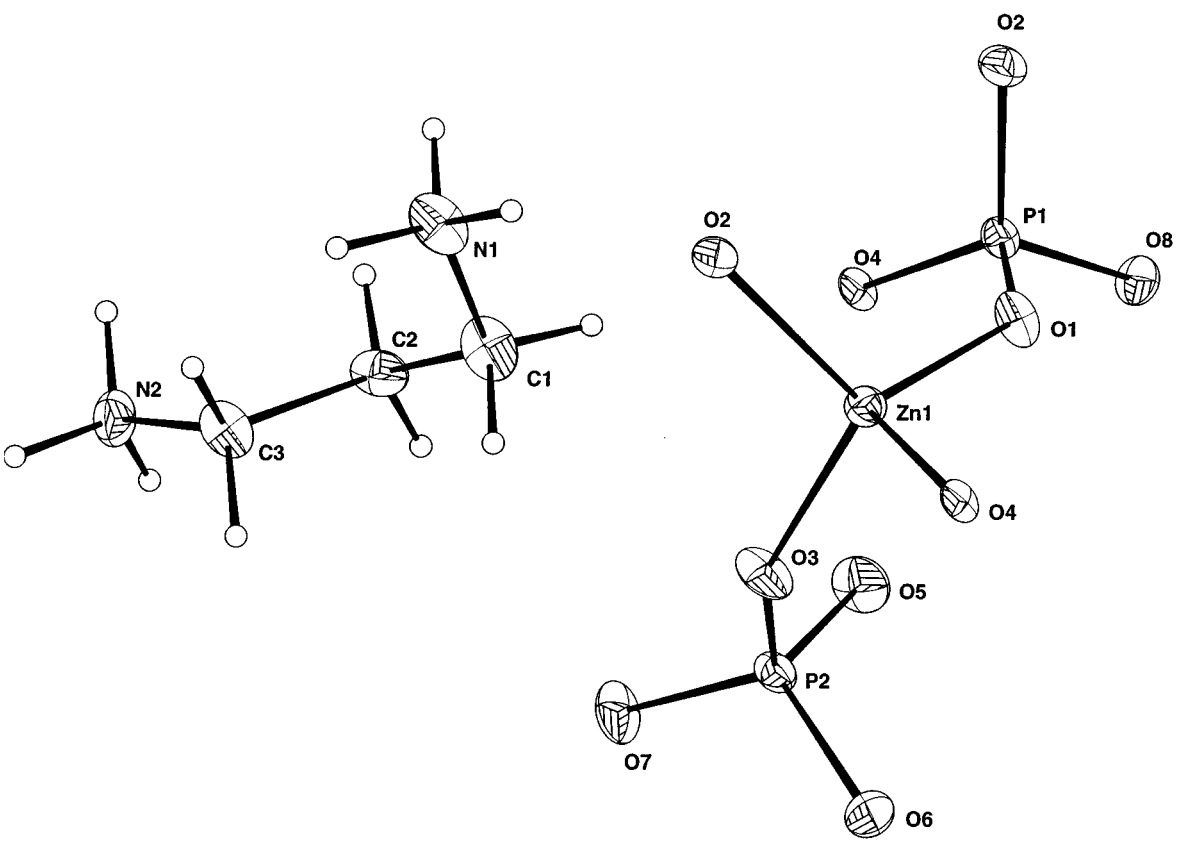


**FIG. 5.** Fragment of the $H_3N(CH_2)_3NH_3 \cdot Zn(HPO_4)_2$ structure showing the atom labelling scheme.

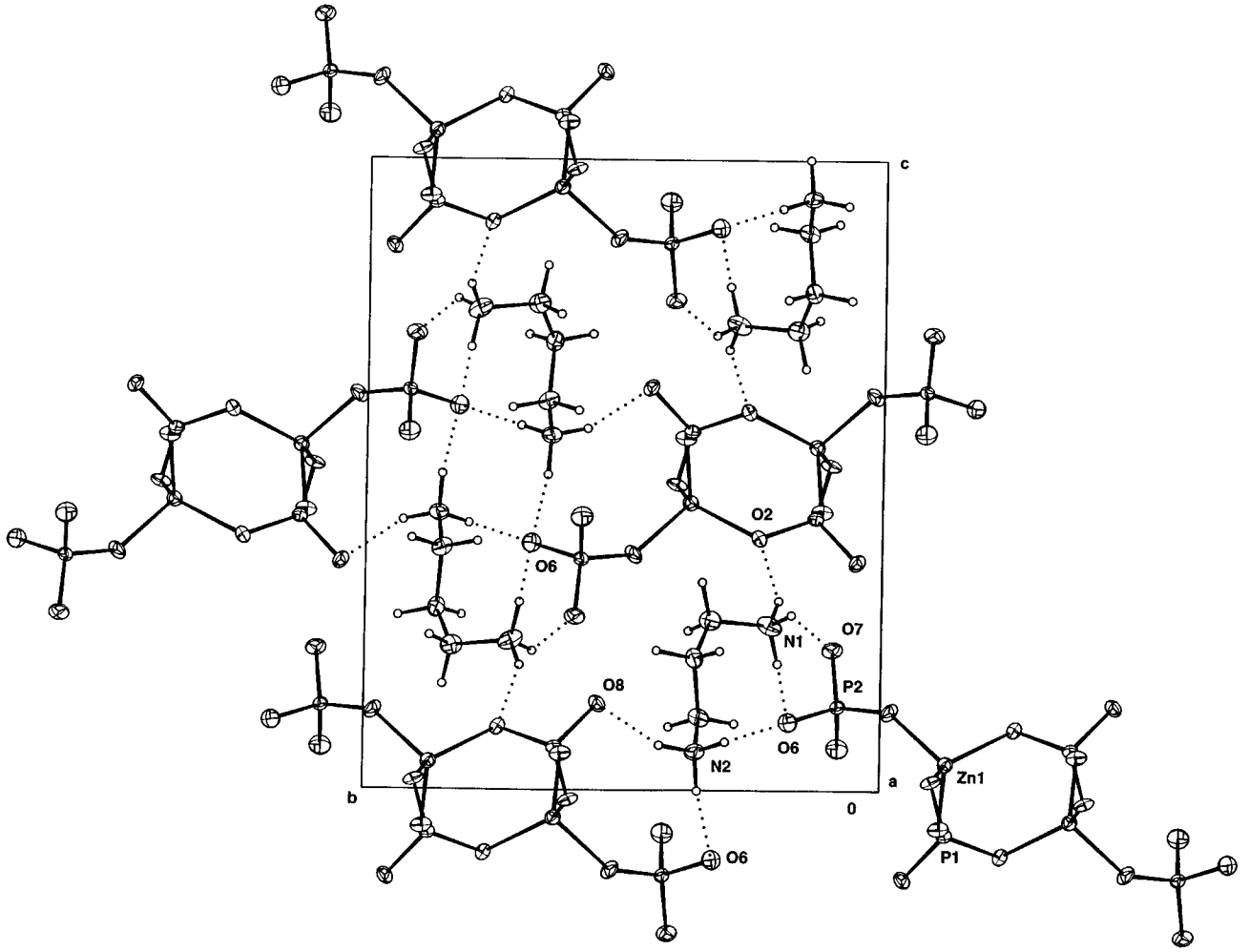


**FIG. 6.** Unit cell packing of $H_3N(CH_2)_3NH_3 \cdot Zn(HPO_4)_2$, viewed down [100]. N–H ··· O hydrogen bonds are indicated by dotted lines. Note the O(6) is an acceptor for three such bonds.

131.3°. There are two distinct P atoms in this phase, both of which adopt typical tetrahedral geometries with $d_{av}$[P(1)–O] = 1.539(3) Å and $d_{av}$[P(2)–O] = 1.540(3) Å. P(1) makes three connections via oxygen to zinc atoms and has one terminal P–O vertex. P(2) makes one P–O–Zn link and has three terminal P–O bonds The charge-balancing criterion requires the presence of two protons associated with the P–O bonds. Bond length–bond strength considerations suggest that the P(1)–O(8) and P(2)–O(5) bonds are protonated, i.e., there are two $HPO_4$ groups in this material. Thus, of the eight distinct O atoms, four are involved in Zn–O–P bridges, two make P–O links and two are parts of P–OH groups.

The $ZnO_4$ and $HPO_4$ groups in $H_3N(CH_2)_3NH_3 \cdot Zn(HPO_4)_2$ fuse together to result in ladder-like one-dimensional chains which propagate along the [100] direction (Fig. 7). These chains are built up from edge-sharing tetrahedral 4-rings, with strictly alternating Zn(1) and P(1) nodes. These 4-ring chains adopt a so-called "double zigzag" geometry (26), akin to the partial tetrahedral connectivity in three-dimensional aluminosilicate zeolites such as the ABW network. In addition, there is a "hanging" $HP(2)O_4$ group attached to each zinc center, resulting in a chain stoichiometry of $[Zn(HPO_4)_2]^{2-}$. There are no P–O–P linkages in this structure, despite the Zn : P ratio of 1 : 2.

As with $H_3N(CH_2)_3NH_3 \cdot Zn_2(HPO_4)_2(H_2PO_4)_2$, template-to-framework hydrogen bonding interactions appear to play an important role in stabilizing the $H_3N(CH_2)_3NH_3 \cdot Zn(HPO_4)_2$ structure. All six N–H vertices make H bonds to zincophosphate chain oxygen atoms which variously form parts of Zn–O–P, P–O, and P–OH groups. The torsion angles of $-66.3°$ for the N(1)–C(1)–C(2)–C(3) and $+167.5°$ for the C(1)–C(2)–C(3)–N(2) groupings of the 1,3-diammonium-propane chain are quite different from those found in $H_3N(CH_2)_3NH_3 \cdot Zn_2(HPO_4)_2(H_2PO_4)_2$.

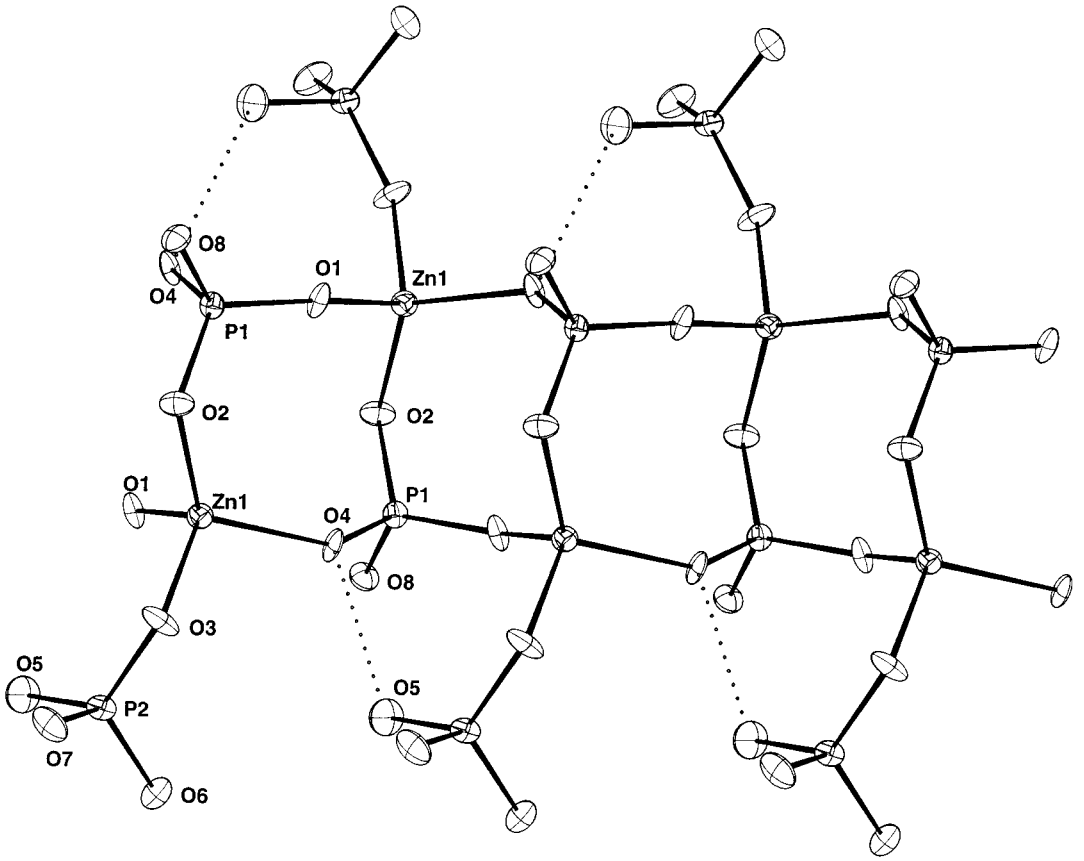


**FIG. 7.** Detail of the $H_3N(CH_2)_3NH_3 \cdot Zn(HPO_4)_2$ structure showing the ladder of edge-sharing tetrahedral 4-rings. Probable O–H ⋯ O-bonding links are indicated by dotted lines. Compare Fig. 1 of ref 25 for the different H-bonding scheme in $C_{10}N_2H_9 \cdot Al(PO_4)(H_2PO_4)$.

*Physical Data*

TGA for $H_3N(CH_2)_3NH_3 \cdot Zn_2(HPO_4)_2(H_2PO_4)_2$ showed a multistep weight loss of 26.1% over the temperature range ~75–650°C. TGA for $H_3N(CH_2)_3NH_3 \cdot Zn(HPO_4)_2$ showed a gradual weight loss of 35.9% over the broad temperature range ~180–750°C.

## DISCUSSION

Two new 1,3-diammonium-propane zincophosphates, $H_3N(CH_2)_3NH_3 \cdot Zn_2(HPO_4)_2(H_2PO_4)_2$ and $H_3N(CH_2)_3NH_3 \cdot Zn(HPO_4)_2$, have been prepared as single crystals and structurally characterized by diffraction methods. They consist of the expected polyhedral units of $ZnO_4$ and $(H_2/H)PO_4$ tetrahedra, sharing vertices. Only Zn–O–P bonds occur as intertetrahedral linkages in these phases, despite the 1 : 2 Zn : P atomic ratio found in each phase. The unpredictable nature of kinetically controlled, solution-mediated synthesis is well illustrated by the fact that two quite dissimilar phases were produced by variants of essentially the same reaction. It would be optimistic to claim any significant degree of *control* over such synthetic procedures at this stage. One reason for this is the "floppy" nature of the templating cation used here. The chain torsion angles of the 1,3-diammonium-propane molecules in these two structures are quite different and are both far removed from the near "ideal" configuration (torsion angles of $-179°$ and $+179°$) of the same molecule in $H_3N(CH_2)_3NH_3 \cdot (H_2PO_4)_2$ (27), where N–H ⋯ O hydrogen bonds are a prominent structural feature. We note also that the higher pressure preparation led to $H_3N(CH_2)_3NH_3 \cdot Zn(HPO_4)_2$, the significantly less dense phase (Table 3).

$H_3N(CH_2)_3NH_3 \cdot Zn_2(HPO_4)_2(H_2PO_4)_2$ is closely related to the layered sodium zinc phosphate hydrate $Na_2Zn(HPO_4)_2 \cdot 4H_2O$ (25), which has an identical sheet topology of bifurcated 12-rings (i.e., 12-rings containing 4-ring groupings) maintaining strict Zn–P alternation. However, in the sodium-containing phase, the 12-rings are considerably less squashed (atom-to-atom dimensions: $\sim 4.4 \times 12.7$ Å for the organic phase; $\sim 9.0 \times 9.2$ Å for the sodium phase). In $Na_2Zn(HPO_4)_2 \cdot 4H_2O$, water molecules

and sodium cations provide the interlayer connectivity, akin to the role of the organic cations found in $H_3N(CH_2)_3NH_3 \cdot Zn_2(HPO_4)_2(H_2PO_4)_2$. Thus, the templating of this distinctive bifurcated 12-ring zincophosphate topology is certainly not the sole preserve of organic cations.

$H_3N(CH_2)_3NH_3 \cdot Zn(HPO_4)_2$ is an unusual one-dimensional zincophosphate. The chain topology of edge-sharing 4-rings has not been observed previously in zincophosphates, $H_3N(CH_2)_3NH_3 \cdot Zn(HPO_4)_2$ is closely related to the recently reported one-dimensional organoaluminophosphate $C_{10}N_2H_9 \cdot Al(PO_4)(H_2PO_4)$ (28), which has an essentially identical chain topology of edge-sharing $AlO_4$ and $PO_4$ tetrahedra, with "hanging" $H_2PO_4$ groups. However, the intrachain H-bonding schemes for these two phases are probably different (Fig. 7). As noted, the edge-shared 4-ring motif is well known as a subunit in various three-dimensional aluminosilicate structures (26).

## ACKNOWLEDGMENT

We thank the Australian Research Council for financial support.

## REFERENCES

1. W. T. A. Harrison, T. E. Gier, T. E. Martin, and G. D. Stucky, *J. Mater. Chem.* **2,** 175 (1992).
2. W. T. A. Harrison, T. M. Nenoff, M. M. Eddy, T. E. Martin, and G. D. Stucky, *J. Mater. Chem.* **2,** 1127 (1992).
3. T. Song, J. Xu, Y. Zhao, Y. Yue, Y. Xu, R. Xu, N. Hu, G. Wei, and H. Jia, *J. Chem. Soc., Chem. Commun.* 1171 (1994).
4. T. Song, M. B. Hursthouse, J. Chen, J. Xu, K. M. A. Malik, R. H. Jones, R. Xu, and J. M. Thomas, *Adv. Mater.* **6,** 679 (1994).
5. M. Wallau, J. Patarin, I. Widmer, P. Caullet, J. L. Guth, and L. Huve, *Zeolites* **14,** 402 (1994).
6. P. Feng, X. Bu, and G. D. Stucky, *Angew. Chem., Int. Ed. Engl.* **34,** 1745 (1995).
7. X. Bu, P. Feng, and G. D. Stucky, *J. Solid State Chem.* **125,** 243 (1996).
8. R. H. Jones, J. Chen, G. Sankar, and J. M. Thomas, "Zeolites and Microporous Materials: State of the Art 1994," p. 2229. Elsevier, New York, 1994.
9. W. T. A. Harrison and L. Hannooman, *Angew. Chem., Int. Ed. Engl.* **36,** 640 (1997).
10. W. T. A. Harrison and M. L. F. Phillips, *Chem. Commun.* 2771 (1996).
11. W. T. A. Harrison and M. L. F. Phillips, *Chem. Mater.* **9,** 1837 (1997).
12. V. Soghomonian, R. Diaz, R. C. Haushalter, and J. Zubieta, *Angew. Chem., Int. Ed. Engl.* **34,** 223 (1995).
13. K.-H. Li and Y.-F. Huang, *Chem. Commun.* 839 (1997).
14. K. Yvon, W. Jeitschko, and E. Parthe, *J. Appl. Crystallogr.* **10,** 73 (1977).
15. T. J. B. Holland and S. A. T. Redfern, Program UNITCELL, University of Cambridge, U.K.
16. A. Altomare, G. Cascarano, G. Giacovazzo, A. Guagliardi, M. C. Burla, G. Polidori, and M. Camalli, *J. Appl. Crystallogr.* **27,** 435 (1994).
17. D. J. Watkin, J. R. Carruthers, and P. W. Betteridge, "CRYSTALS User Guide," Chemical Crystallography Laboratory, University of Oxford, U.K.
18. "International Tables for Crystallography," Vol. IV. Kynoch Press, Birmingham, U.K., 1974.
19. A. C. Larson, *Acta Crystallogr.* **23,** 664 (1967).
20. H. D. Flack, *Acta Crystallogr. A* **39,** 876 (1983).
21. L. J. Pearce, D. J. Watkin, and C. K. Prout, "CAMERON User Guide," Chemical Crystallography Laboratory, University of Oxford, U.K.
22. P. Lightfoot and D. Masson, *Acta Crystallogr. C* **52,** 1077 (1996).
23. I. D. Brown, Program VALENCE (PC version), Institute for Materials Research, McMaster University, Canada.
24. C. D. Landee and R. D. Willett, *Inorg. Chem.* **20,** 2521 (1981).
25. W. T. A. Harrison, T. M. Nenoff, T. E. Gier, and G. D. Stucky, *J. Solid State Chem.* **113,** 168 (1994).
26. J. V. Smith, *Chem. Rev.* **88,** 149 (1988).
27. S. Kamoun, A. Jouini, A. Daoud, A. Durif, and J.-C. Guitel, *Acta Crystallogr. C* **48,** 133 (1992).
28. A. M. Chippindale and C. Turner, *J. Solid State Chem.* **128,** 318 (1997).